Supplement of Atmos. Chem. Phys., 24, 13793–13810, 2024
https://doi.org/10.5194/acp-24-13793-2024-supplement

*Supplement of*

# Molecular and seasonal characteristics of organic vapors in urban Beijing: insights from Vocus-PTR measurements

**Zhaojin An et al.**

*Correspondence to:* Jingkun Jiang (jiangjk@tsinghua.edu.cn)

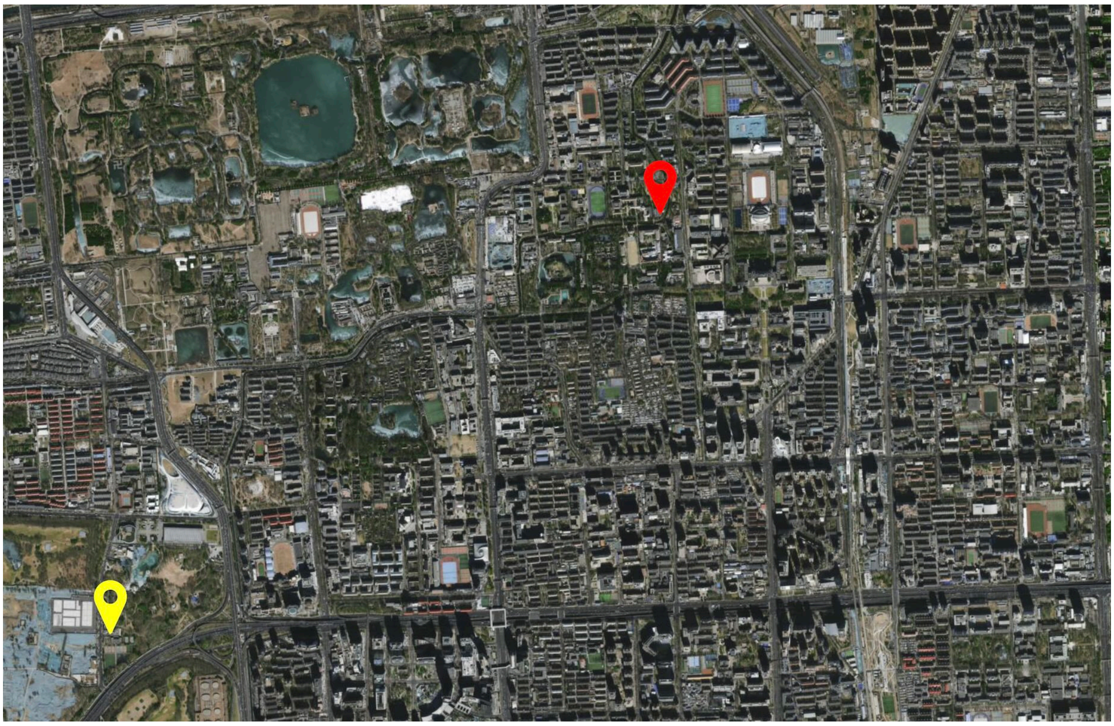

Figure S1. The map of the observation site (© Gaode Maps), labelled in red. The site is approximately 1 kilometer away from the nearby traffic roads. The state-operated air quality station (Wanliu station) is labelled in yellow.

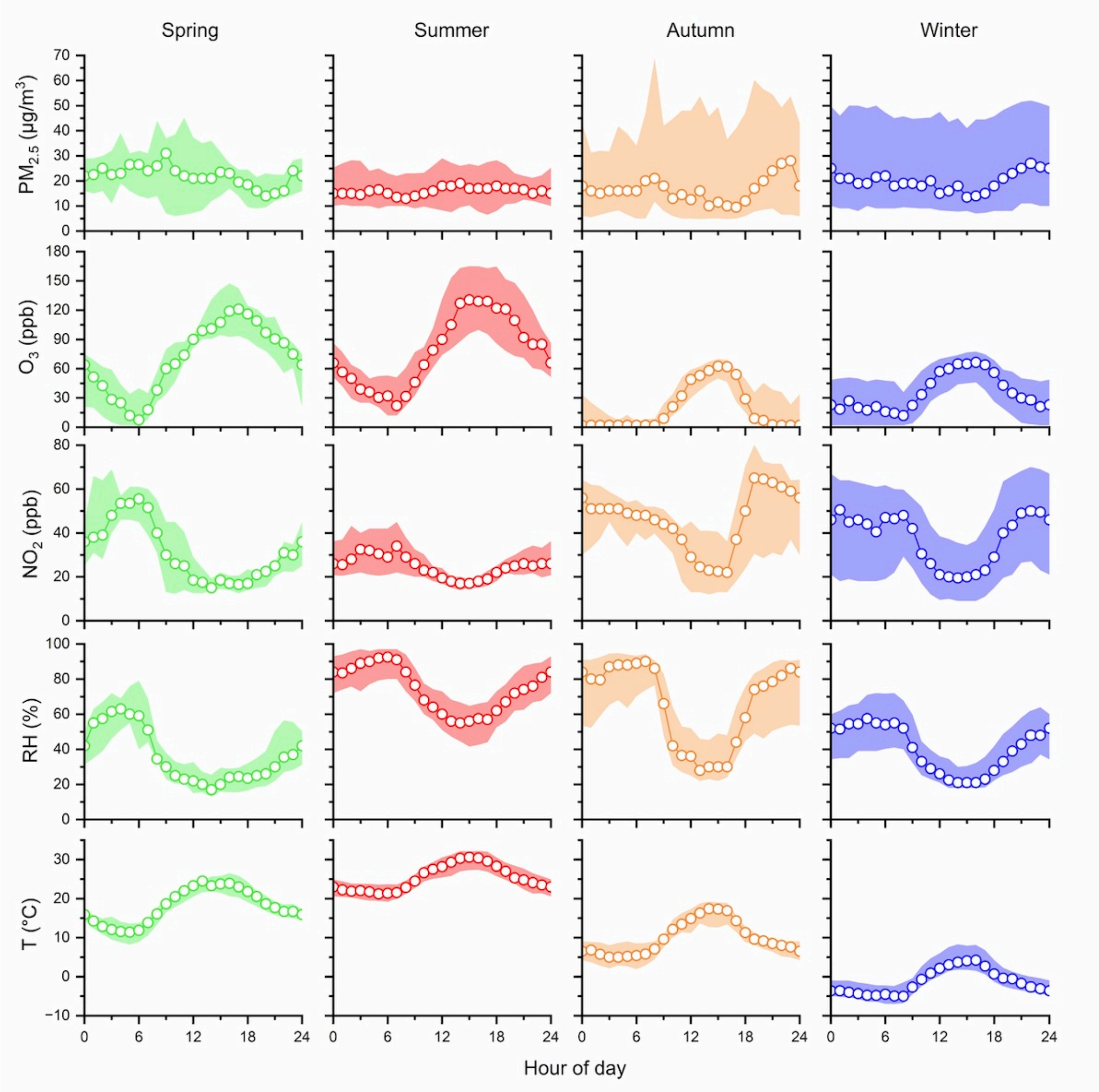

Figure S2. Median diurnal variations of $PM_{2.5}$, $O_3$, $NO_x$ ($NO+NO_2$), relative humidity (RH), and temperature (T) in four seasons. The shaded areas in the graph represent the 25th and 75th percentiles.

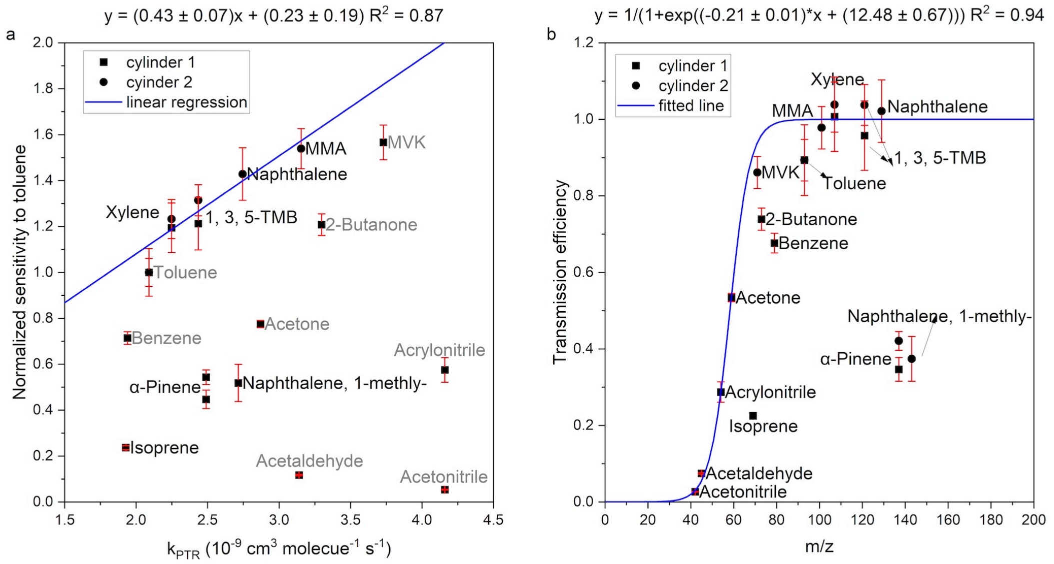

Figure S3. Calibration results of mixed calibration gases. (a) The scatter plot of the sensitivities of mixed calibration gases and their $k_{PTR}$. The blue line is the linear fitting of $C_7H_9^+$, $C_8H_{11}^+$, $C_9H_{13}^+$, $C_{10}H_9^+$, and $C_5H_9O_2^+$, respectively. The error bar refers to standard deviation. The sensitivities of species with gray labels are affected by transmission. (b) The transmission efficiency of mixed calibration gases. The blue line is the fitted transmission efficiency curve based on that of mixed calibration gases. The error bar refers to standard deviation.

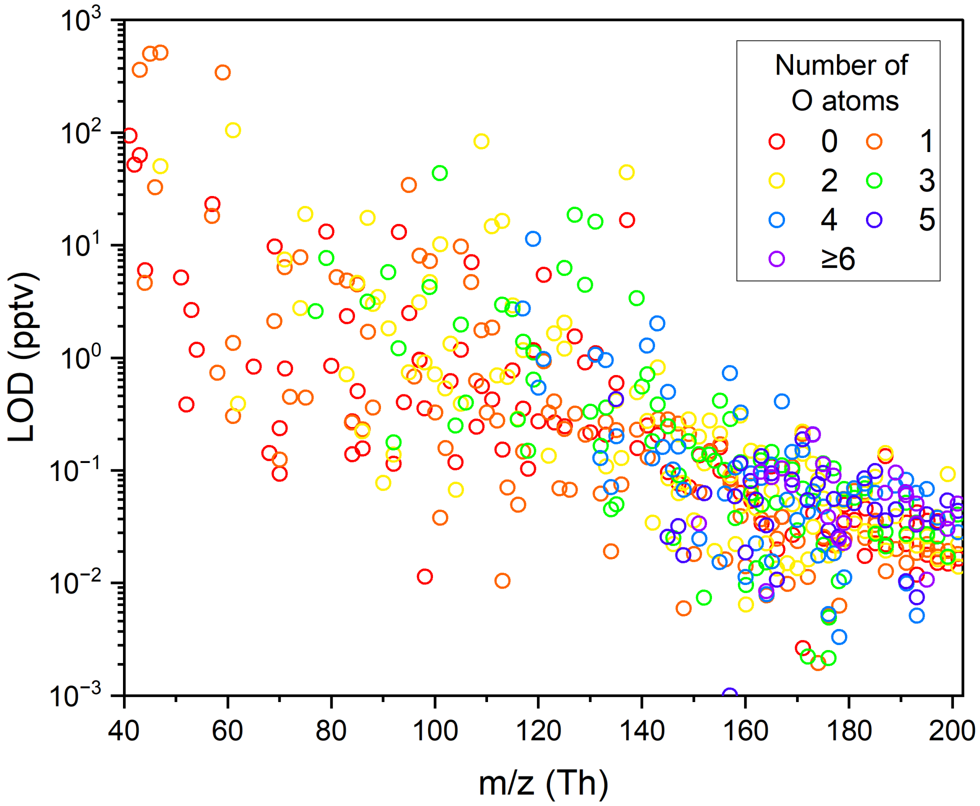

Figure S4. Average limits of detection (1 min) for detected compounds. Different colors refer to different oxygen number of compounds, as labelled in legend.

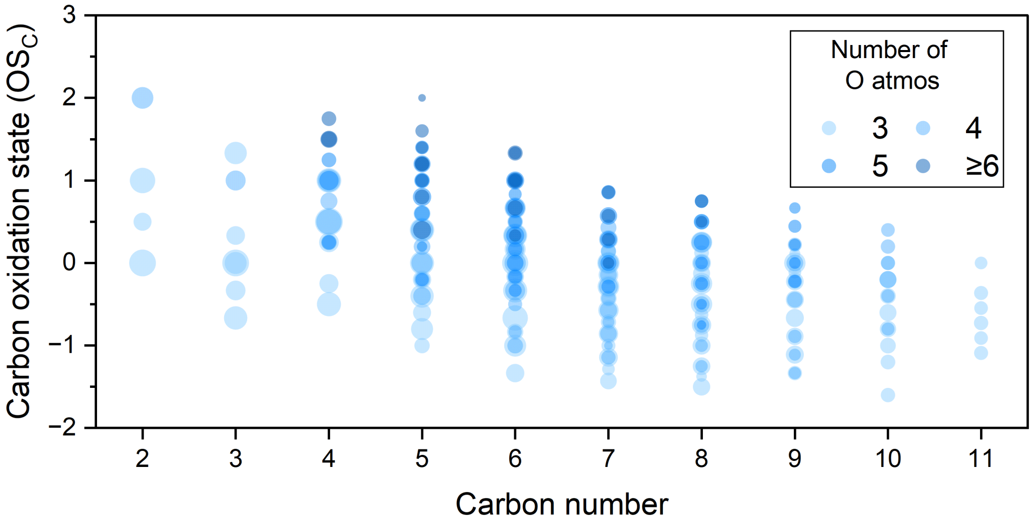

Figure S5. Carbon oxidation state of organic vapors with different oxygens. The sizes of the bubbles are determined by the annual median mixing ratios. The bubbles are colored by different oxygen numbers as labeled in the legend. Bars labeled as 6 refers to organic vapors with oxygen number equal or larger than 6.

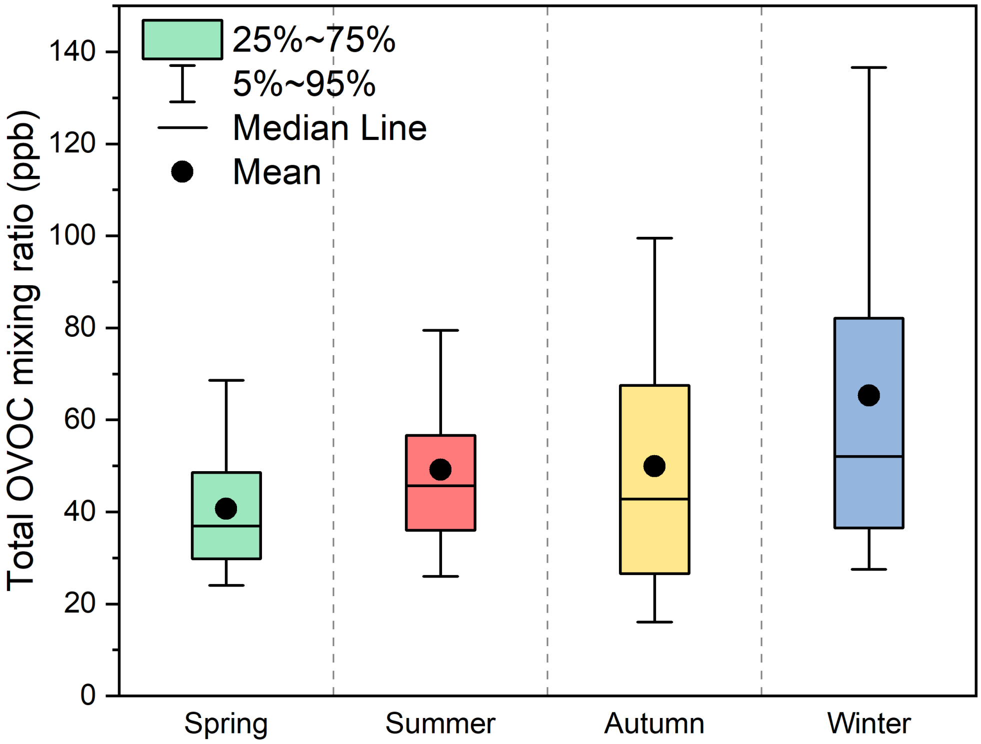

Figure S6. Boxplot of total OVOC mixing ratios in four seasons.

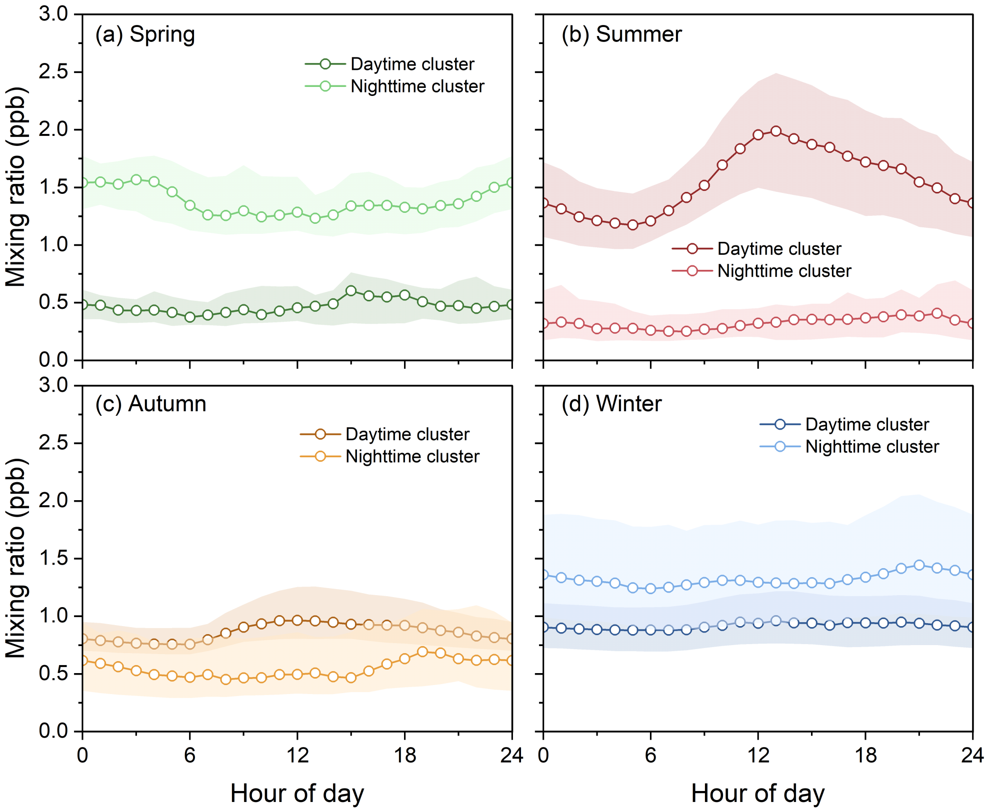

Figure S7. Diurnal variation cluster results of organic vapors with multiple oxygens. Median mixing ratios are presented. The shaded areas in the graph are 25th and 75th percentiles. The colors of the clusters are consistent with Figure 5. (a) Spring. (b) Summer. (c) Autumn. (d) Winter.

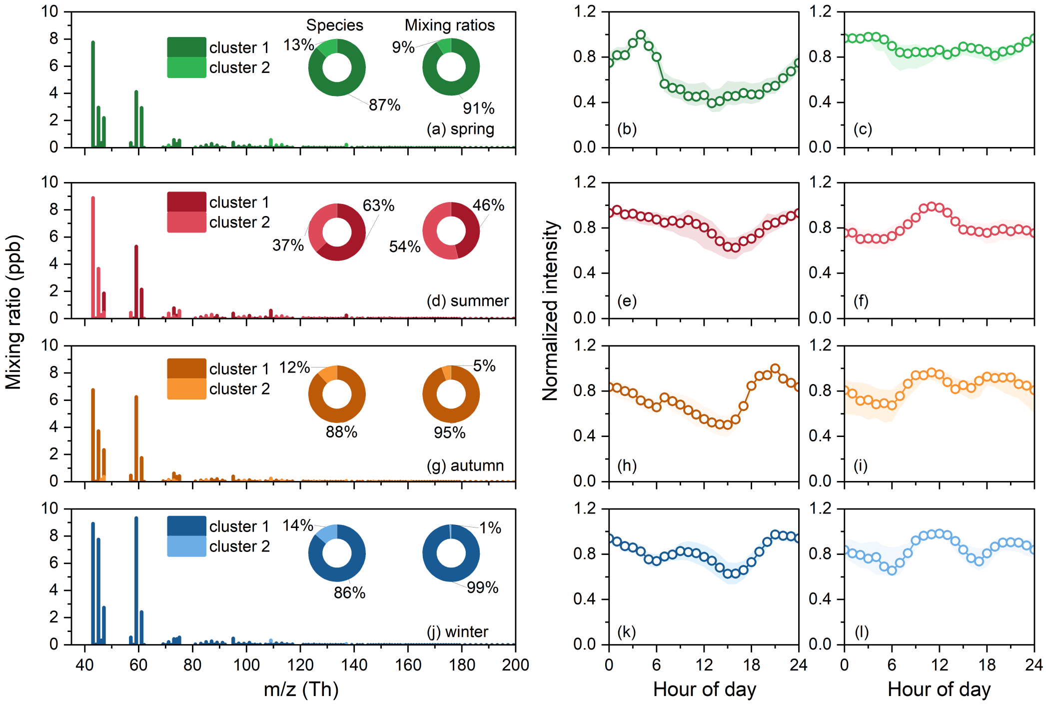

Figure S8. Cluster results of organic vapors with one or two oxygens. (a) – (c) Cluster results for spring. (a) Mass spectra of organic vapors with one or two oxygens in spring. Y axis is the mean mixing ratio of each compound. Two different shades of colors are used to distinguish between two clusters. Two pie charts represent the distribution of species numbers and mixing ratios of for two clusters. (b) Normalized median diurnal variation of cluster 1. (c) Normalized median diurnal variation of cluster 2. The shaded areas in the graph (b) and (c) represent the 25th and 75th percentiles. (d) – (f) Cluster results for summer. (g) to (i) Cluster results for autumn. (j) – (l) Cluster results for winter.

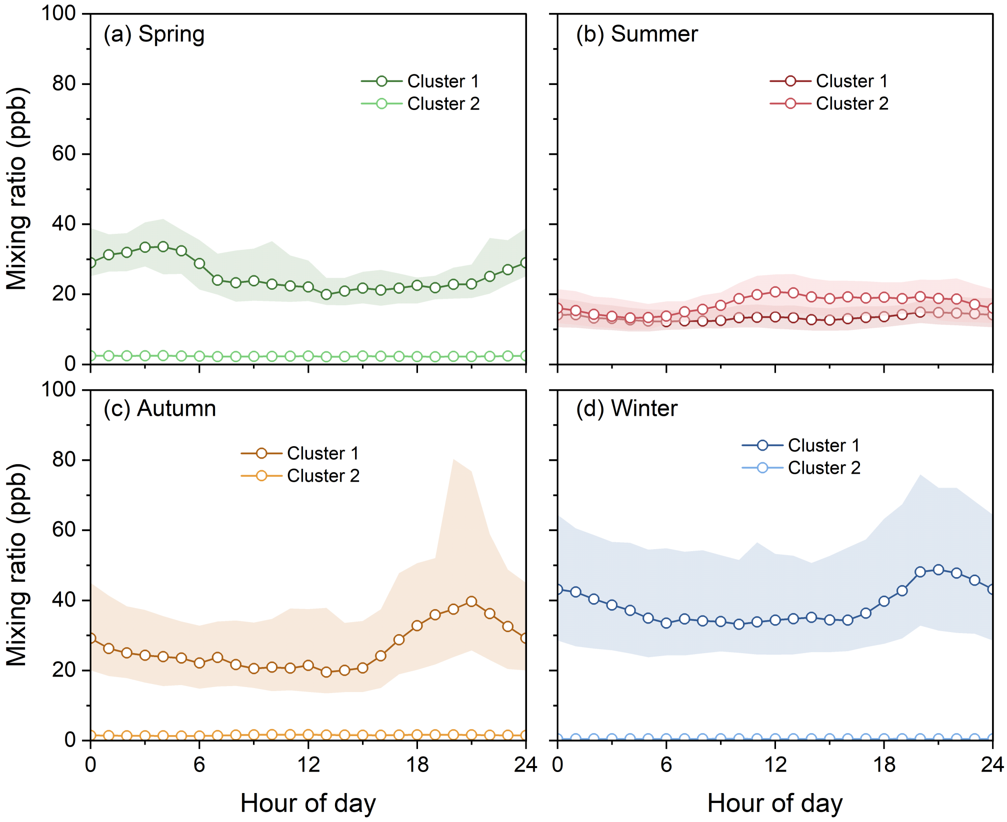

Figure S9. Diurnal variation cluster results of organic vapors with one or two oxygens. Median mixing ratios are presented. The shaded areas in the graph are 25th and 75th percentiles. The colors of the clusters are consistent with Figure S8. (a) Spring. (b) Summer. (c) Autumn. (d) Winter.

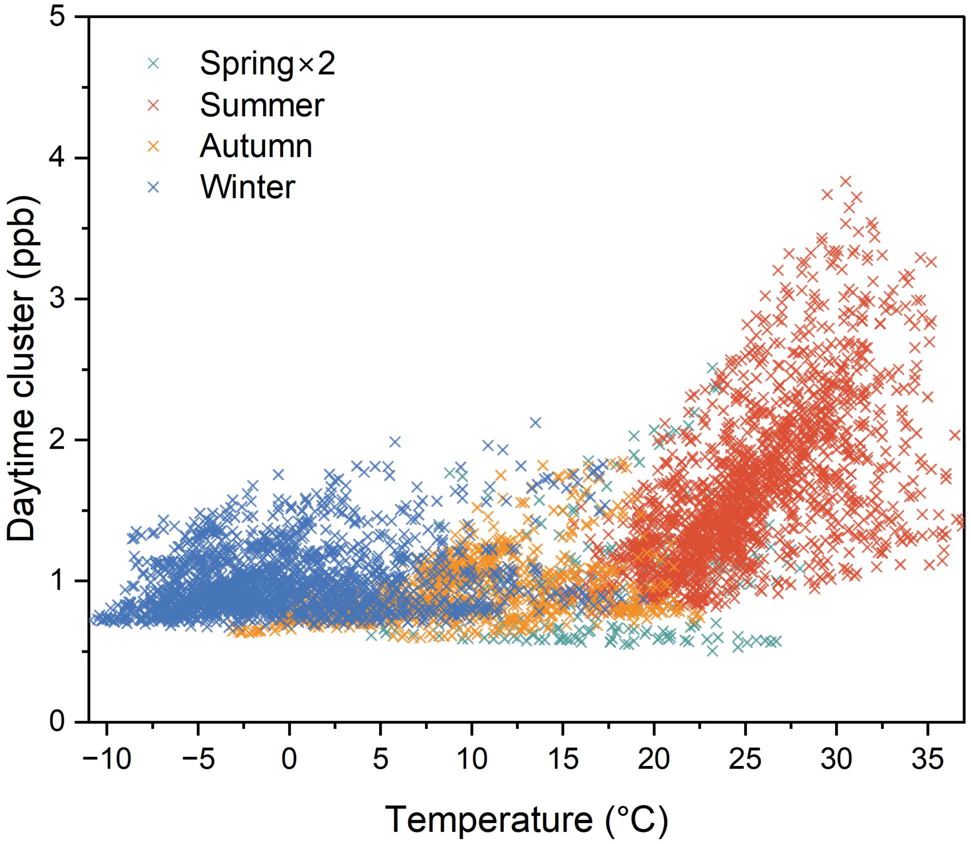

Figure S10. Dependence of the sum of daytime clusters on temperature.

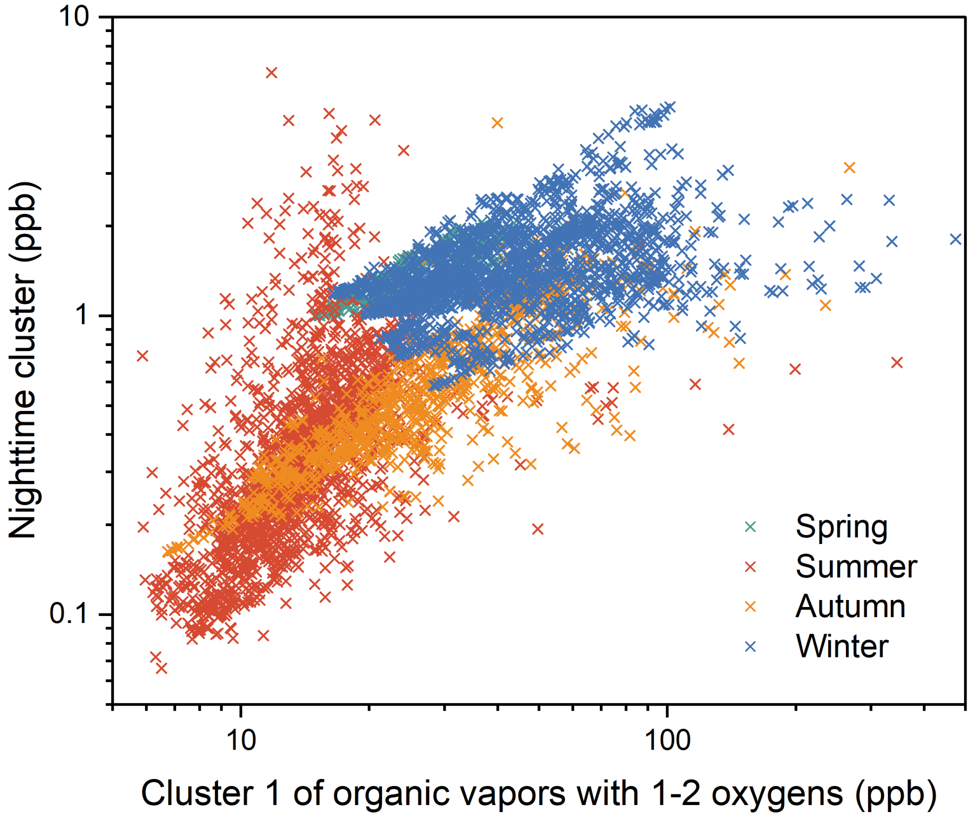

Figure S11. Dependence of the sum of nighttime clusters on the sum of cluster 1s of organic vapors with 1-2 oxygens.

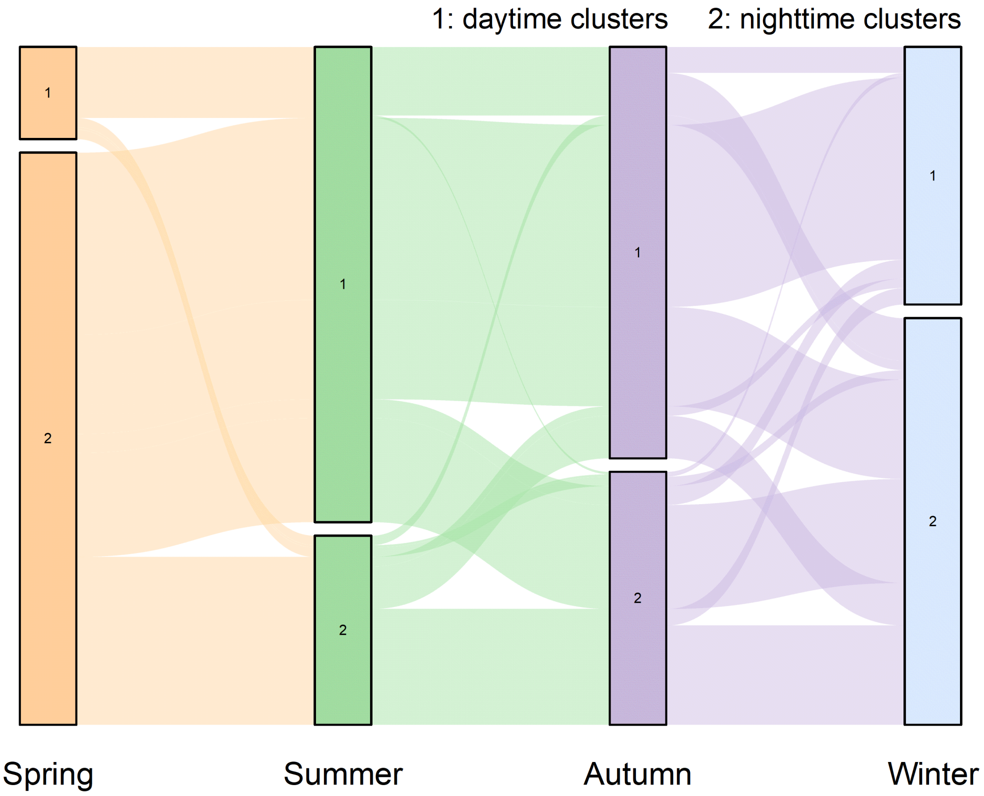

Figure S12. The distribution of organic vapors with multiple oxygens across different clusters.

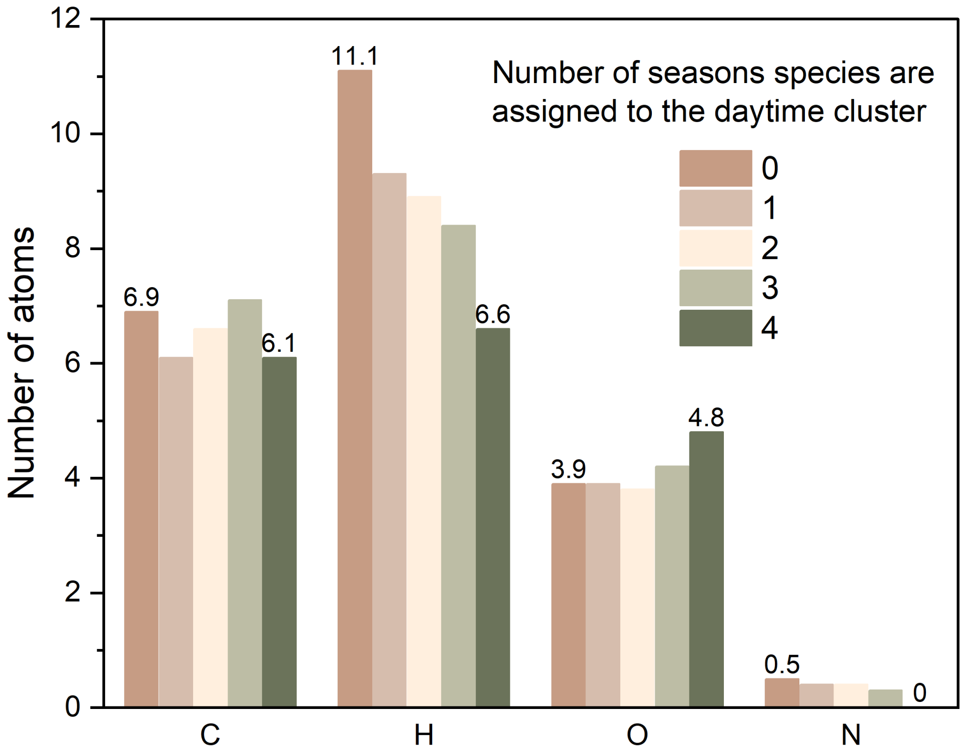

Figure S13. The average number of C, H, O, and N atoms in organic vapors containing multiple oxygen atoms, categorized by how often they are assigned to the daytime cluster across the four seasons. The categories are based on the frequency of assignment, with the number n (0-4) indicating the number of seasons in which the species are classified into the daytime cluster.

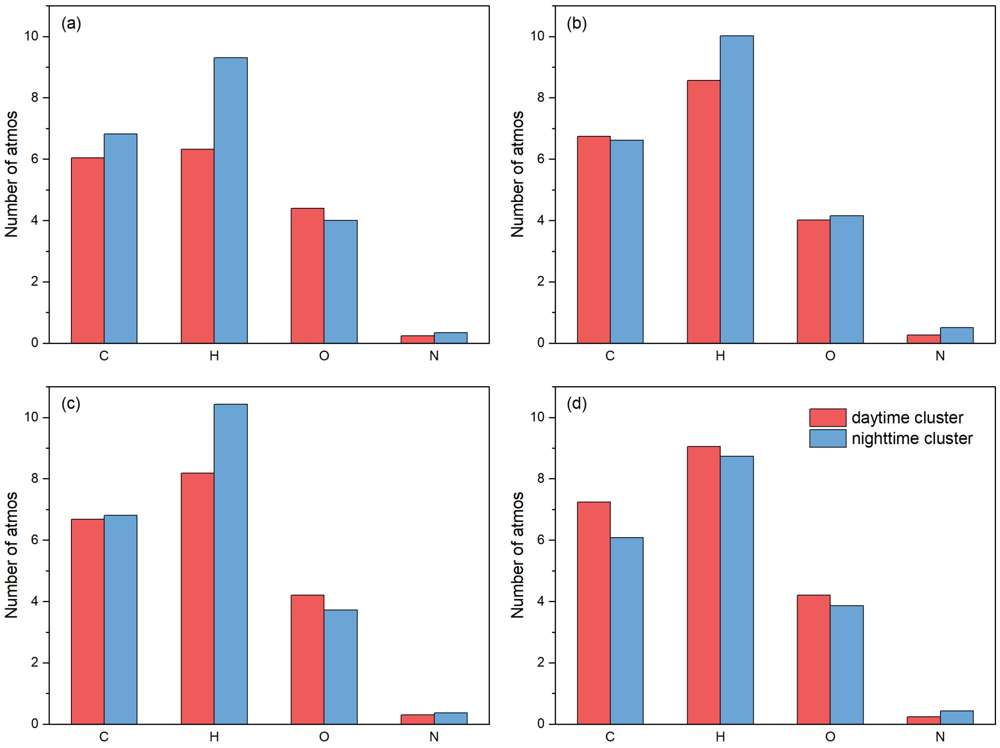

Figure S14. Average C, H, O, and N number of organic vapors containing multiple oxygens in two clusters. (a) Spring. (b) Summer. (c) Autumn. (d) Winter.

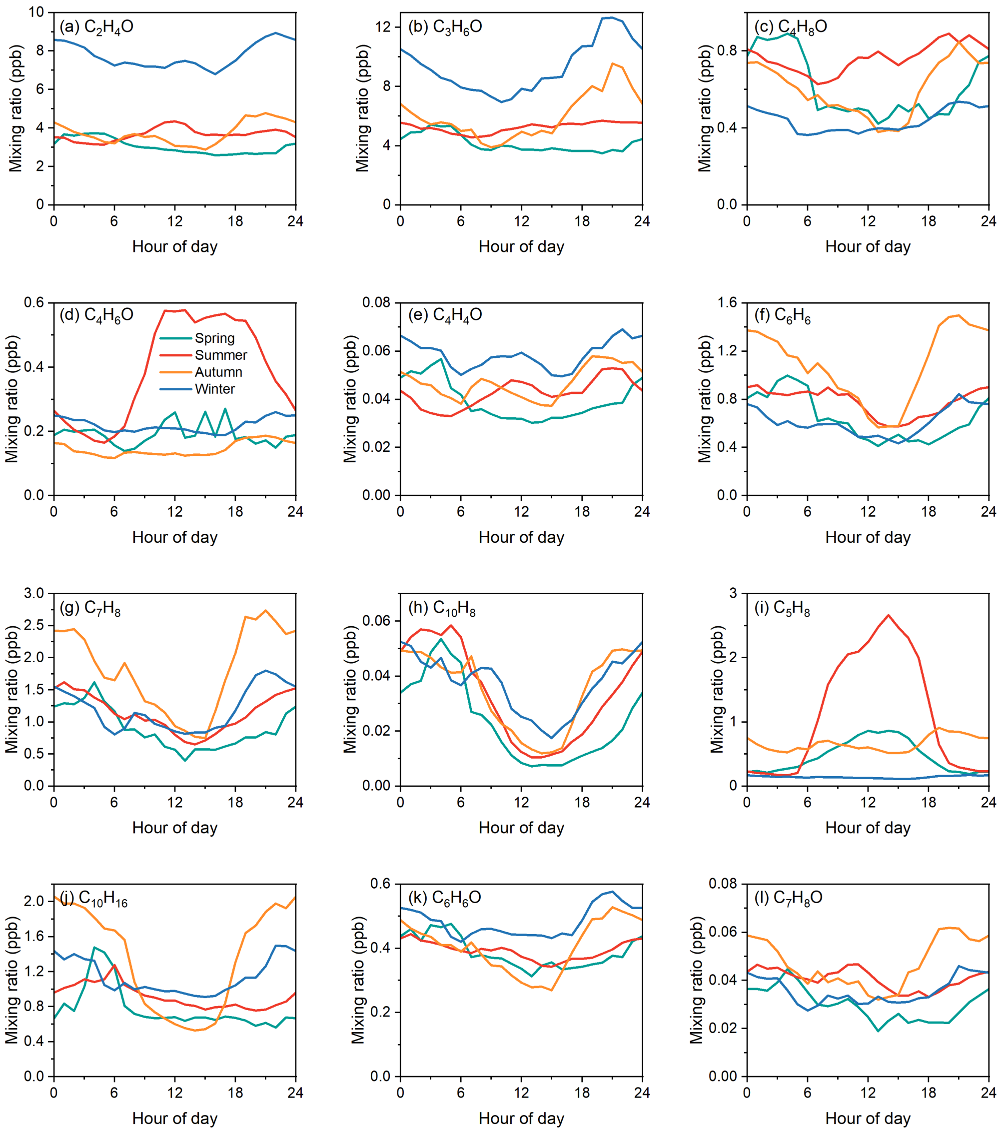

Figure S15. Diurnal profiles of representative VOCs in four seasons. Median mixing ratios are used. The green line represents spring, the red line represents summer, the orange line represents autumn, and the blue line represents winter.

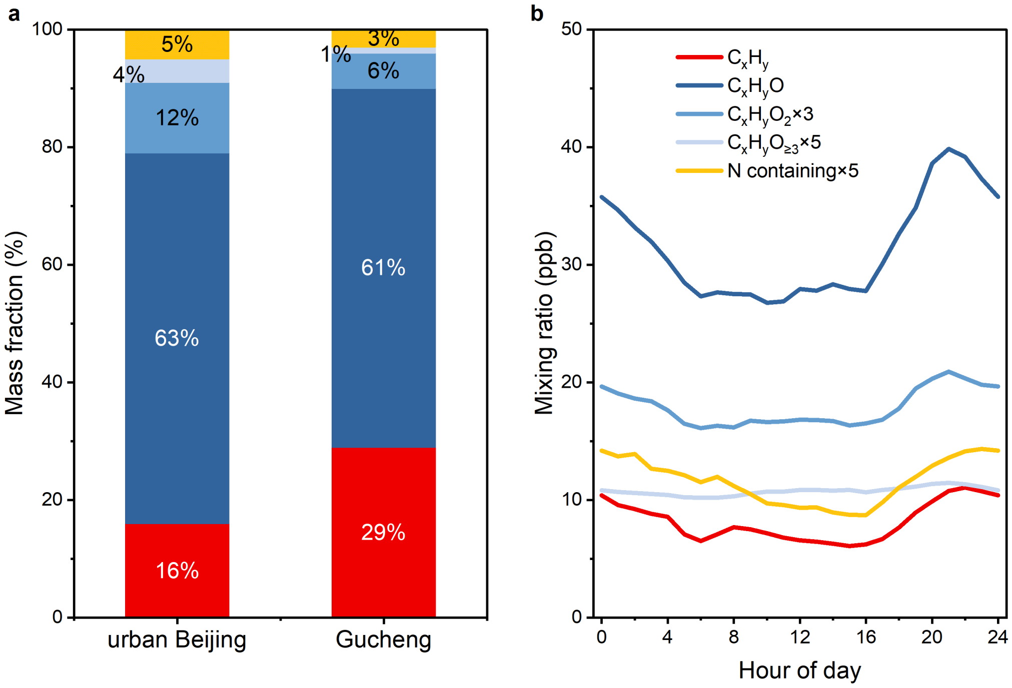

Figure S16. (a) Mass fraction of different categories. Only winter results are used here for urban Beijing. Gucheng results are measured in winter 2018 from He et al., 2022. (b) Diurnal Pattern of different categories in winter.

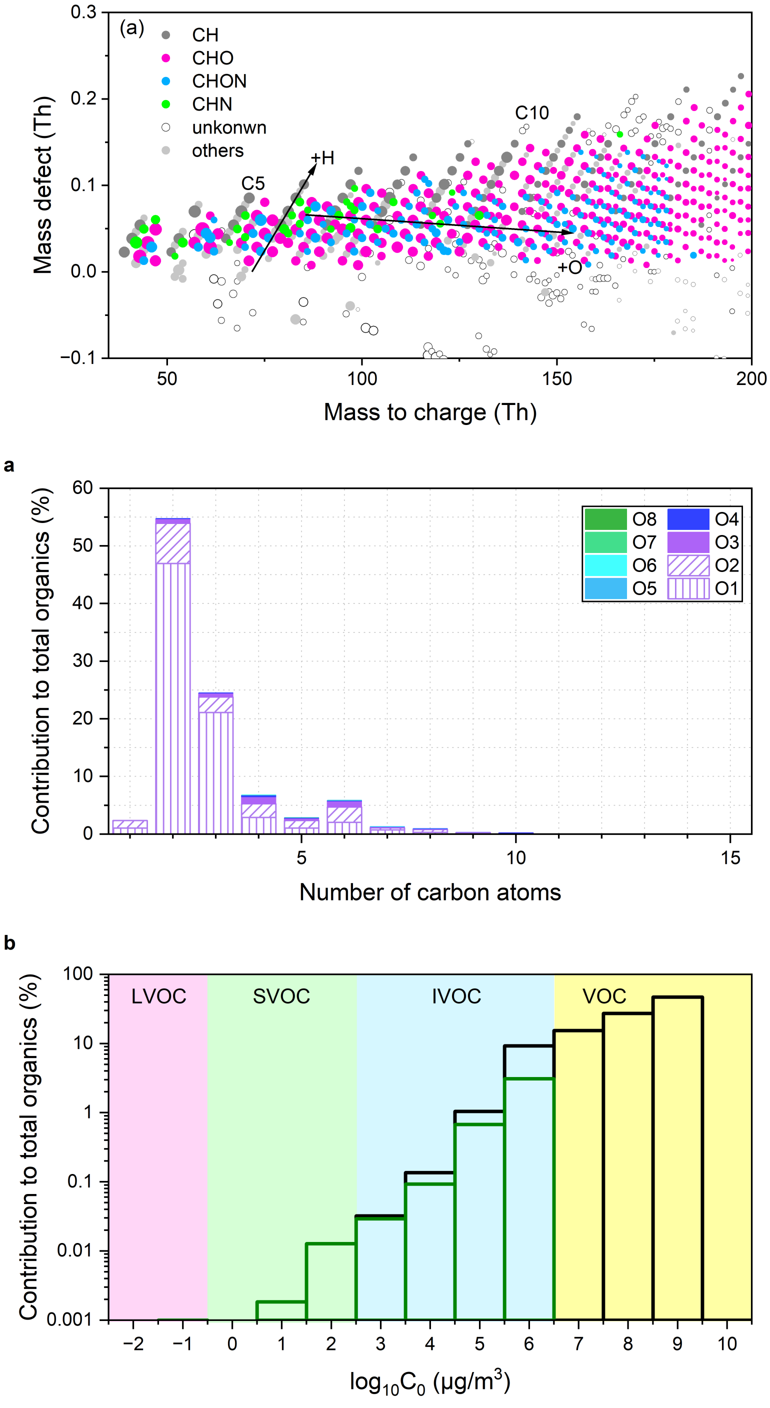

Figure S17. Molecular characteristics of total measured organic vapors by Vocus-PTR. (a) Carbon number distribution. Different colors and patterns of bars refer to compounds with different oxygens. Annual median mixing ratios are used to calculate the contribution to total organics. (b) Volatility distribution. Bars with black borders represent total measured organic vapors by Vocus-PTR. Bars with green borders represent organic vapors with multiple oxygens (≥3). Annual median mixing ratios are used to calculate the contribution to total organics.

Table S1. The observation periods of Vocus-PTR

| Period NO. | Start time | End time | Season |
|---|---|---|---|
| 1 | 5/1/2021 | 5/11/2021 | Spring |
| 2 | 6/11/2021 | 7/12/2021 | Summer |
| 3 | 7/27/2021 | 9/8/2021 | Summer |
| 4 | 10/11/2021 | 11/16/2021 | Autumn |
| 5 | 12/27/2021 | 3/10/2022 | Winter |

Table S2. Information about calibration gases

| Name | Formula | Mixing ratio (ppb) | Observation periods |
|---|---|---|---|
| Acetonitrile | $C_2H_3N$ | 8.16 | 1-4 |
| Acetaldehyde | $C_2H_4O$ | | |
| Acrylonitrile | $C_3H_3N$ | | |
| Acetone | $C_3H_6O$ | | |
| Isoprene | $C_5H_8$ | | |
| 2-Butanone | $C_4H_8O$ | | |
| Benzene | $C_6H_6$ | | |
| Toluene | $C_7H_8$ | | |
| Xylene | $C_8H_{10}$ | | |
| 1, 3, 5-Trimethylbenze | $C_9H_{12}$ | | |
| α-Pinene | $C_{10}H_{16}$ | | |
| Methyl vinyl ketone | $C_4H_6O$ | 20 | 5 |
| Methyl methacrylate | $C_5H_8O_2$ | | |
| Toluene | $C_7H_8$ | | |
| Xylene | $C_8H_{10}$ | | |
| α-Pinene | $C_{10}H_{16}$ | | |
| 1, 3, 5-Trimethylbenze | $C_9H_{12}$ | | |
| Naphthalene | $C_{10}H_8$ | | |
| Naphthalene, 1-methly- | $C_{11}H_{10}$ | | |

Table S3. Corrected fragments and water clusters in Vocus-PTR

| Parent ion | Derivative ion | Type |
|---|---|---|
| $C_2H_4N^+$ | $C_2H_6NO^+$ | Water cluster |
| $C_3H_7O^+$ | $C_3H_9O_2^+$ | Water cluster |
| $C_5H_9^+$ | $C_5H_7^+$ | Fragment |
| $C_7H_9^+$ | $C_7H_7^+$ | Fragment |
| $CH_4NO^+$ | $CH_6NO_2^+$ | Water cluster |
| $C_2H_7O^+$ | $C_2H_9O_2^+$ | Water cluster |
| $C_3H_3O_2^+$ | $C_3H_5O_3^+$ | Water cluster |
| $C_4H_5O_2^+$ | $C_4H_7O_3^+$ | Water cluster |
| $C_3H_5^+$ | $C_3H_3^+$ | Fragment |
| $C_2H_5O^+$ | $C_2H_7O_2^+$ | Water cluster |
| $C_2H_4NO^+$ | $C_2H_6NO_2^+$ | Water cluster |
| $C_4H_5O_2^+$ | $C_4H_7O_3^+$ | Water cluster |
| $C_3H_3O_3^+$ | $C_3H_5O_4^+$ | Water cluster |
| $C_6H_6NO^+$ | $C_6H_8NO_2^+$ | Water cluster |
| $C_8H_8NO_2^+$ | $C_8H_{10}NO_3^+$ | Water cluster |
| $C_{10}H_{21}O^+$ | $C_{10}H_{23}O_2^+$ | Water cluster |
| $C_9H_{13}O_3^+$ | $C_9H_{15}O_4^+$ | Water cluster |
| $C_{10}H_{13}O_3^+$ | $C_{10}H_{15}O_4^+$ | Water cluster |
| $C_{14}H_{13}^+$ | $C_{14}H_{15}O^+$ | Water cluster |

Table S4. Main $C_xH_yO_{\geqslant 3}$ and $C_xH_yO_{\geqslant 3}N$ species measured in this study

| DBE | CHO | CHON |
|---|---|---|
| 0 | $C_nH_{2n+2}O_{3,4}$ | |
| 1 | $C_nH_{2n}O_{3\text{-}8}$ | $C_nH_{2n+1}O_{3\text{-}5}N$ |
| 2 | $C_nH_{2n-2}O_{3\text{-}6}$ | $C_nH_{2n-1}O_{3\text{-}5}N$ |
| 3 | $C_nH_{2n-4}O_{3\text{-}8}$ | $C_nH_{2n-3}O_{3\text{-}6}N$ |
| 4 | $C_nH_{2n-6}O_{3\text{-}7}$ | $C_nH_{2n-5}O_{3\text{-}6}N$ |
| 5 | $C_nH_{2n-8}O_{3\text{-}6}$ | $C_nH_{2n-7}O_{3\text{-}5}N$ |
| 6 | $C_nH_{2n-10}O_{3\text{-}6}$ | $C_nH_{2n-9}O_{3,4}N$ |
| 7 | $C_nH_{2n-12}O_{3\text{-}5}$ | $C_nH_{2n-11}O_3N$ |
| 8 | $C_nH_{2n-14}O_{3\text{-}5}$ | $C_nH_{2n-13}O_3N$ |
| 9 | $C_nH_{2n-16}O_{3,4}$ | |

Table S5. Seasonal mixing ratios of OVOCs with multiple oxygens

| Category | | | Spring | Summer | Autumn | Winter |
|---|---|---|---|---|---|---|
| O = 3 | CHO | mean | 1599.3 | 1756.0 | 1342.2 | 2047.5 |
| | | median | 1524.1 | 1497.8 | 1138.8 | 1796.5 |
| | CHON | mean | 33.6 | 53.6 | 36.5 | 46.5 |
| | | median | 30.1 | 48.0 | 28.7 | 38.2 |
| O = 4 | CHO | mean | 199.4 | 178.7 | 176.4 | 328.5 |
| | | median | 194.2 | 163.4 | 163.7 | 328.0 |
| | CHON | mean | 14.3 | 18.3 | 13.1 | 18.9 |
| | | median | 12.4 | 16.4 | 10.9 | 16.7 |
| O = 5 | CHO | mean | 20.1 | 25.2 | 15.9 | 18.5 |
| | | median | 18.1 | 23.5 | 14.9 | 17.3 |
| | CHON | mean | 8.8 | 5.5 | 1.7 | 1.7 |
| | | median | 7.1 | 4.8 | 1.5 | 1.3 |
| O ≥ 6 | CHO | mean | 9.0 | 10.5 | 5.9 | 5.0 |
| | | median | 8.0 | 9.3 | 4.9 | 4.2 |
| | CHON | mean | 1.0 | 1.7 | 0.5 | 0.3 |
| | | median | 0.8 | 1.5 | 0.4 | 0.2 |

Units in ppt.

Section S1. Calculation methods of double bond equivalent (DBE), carbon oxidation state ($\overline{OS}_C$), and volatility.

DBE is calculated as follows:

$$DBE = n_C + 1 - 0.5 \times n_H + 0.5 \times n_N \qquad (1)$$

Where $n_C$, $n_H$, and $n_N$ are the number of carbon, hydrogen, and nitrogen atoms of organic vapors, respectively. $\overline{OS}_C$ is calculated as follows (Kroll et al., 2011):

$$\overline{OS}_C = 2 \times n_O / n_C - n_H / n_C \qquad (2)$$

Where $n_C$, $n_O$, and $n_H$ are the number of carbon, oxygens, and hydrogen atoms of organic vapors, respectively. The saturation mass concentration $C_0$, calculated using parameterization method by Li et al. (Li et al., 2016), are used to describe the volatility of organic vapors, as given below:

$$log_{10}C_0 = (n_C^0 - n_C)b_c - n_O b_O - 2\frac{n_C n_O}{n_C + n_O} b_{CO} - n_N b_N \qquad (3)$$

Where $n_C^0$ is the reference carbon number; $n_C$, $n_O$, and $n_N$ are the number of carbon, oxygen, and nitrogen atoms of organic vapors, respectively; $b_c$, $b_O$, and $b_N$ are the contribution of carbon, oxygen, and nitrogen atom to $log_{10}C_0$, respectively; $b_{CO}$ is the carbon-oxygen nonideality.

References:

Kroll, J. H., Donahue, N. M., Jimenez, J. L., Kessler, S. H., Canagaratna, M. R., Wilson, K. R., Altieri, K. E., Mazzoleni, L. R., Wozniak, A. S., Bluhm, H., Mysak, E. R., Smith, J. D., Kolb, C. E., and Worsnop, D. R.: Carbon oxidation state as a metric for describing the chemistry of atmospheric organic aerosol, Nature Chemistry, 3, 133-139, 10.1038/nchem.948, 2011.

Li, Y., Pöschl, U., and Shiraiwa, M.: Molecular corridors and parameterizations of volatility in the chemical evolution of organic aerosols, Atmos. Chem. Phys., 16, 3327-3344, 10.5194/acp-16-3327-2016, 2016.